Characteristic Time Scales for Predicting the Scalar Flux at a Free Surface in Turbulent Open-Channel Flows

Ryuichi Nagaosa
Research Center for Compact Chemical System (CCS), AIST, Miyagino, Sendai 983-8551, Japan

Center for Environmental Energy Engineering (CEEE), University of Maryland, College Park, MD 20742

Robert A. Handler
Dept. of Mechanical Engineering, Texas A&M University, College Station, TX 77843

DOI 10.1002/aic.13773
Published online March 1, 2012 in Wiley Online Library (wileyonlinelibrary.com).

The purpose of this study is to predict the turbulent scalar flux at a free surface subject to a fully developed turbulent flow based on a hydrodynamic analysis of turbulence in the region close to the free surface. The effect of the Reynolds number on turbulent scalar transfer mechanisms is extensively examined. A direct numerical simulation technique is applied to achieve the purpose. The surface-renewal approximation is used to correlate the free-surface hydrodynamics and scalar transport at the free surface. Two types of characteristic time scales have been examined for predicting turbulent scalar flux. One is the time scale derived from the characteristic length and velocity scale at the free surface. The other is the reciprocal of the root-mean-square surface divergence. The results of this study show that scalar transport at the free surface can be predicted successfully using these time scales based on the concept of the surface-renewal approximation. © 2012 American Institute of Chemical Engineers *AIChE J,* 58: 3867–3877, 2012
Keywords: computational fluid dynamics, fluid mechanics, scalar transfer, turbulence, interfacial processes

Introduction

Understanding scalar transport mechanisms at a free surface contributes to the establishment of a predictive model for turbulent scalar exchange between gas and liquid phases. These models are useful in evaluating exchange rates of active and passive scalars at the sea surface between the turbulent ocean and atmosphere. The scalar transfer processes between gas and liquid provide significant amounts of data on the design and manipulation of engineering equipment such as cooling towers and heat exchangers.

It is widely known that turbulence quantities beneath the free surface determine the turbulent scalar flux, because the molecular diffusivity of most scalars in water is much smaller than in air. The authors have studied turbulence scalar transfer mechanisms in a turbulent open-channel flow based on laboratory and numerical experiments.[1–6] The results of these studies have revealed that turbulent vortical structures produced in the turbulent boundary layer travel toward the free surface and interact with it. These interactions replace fluid elements at the free surface with fluid from the bulk, enhancing the flux there. For this reason, they are often referred to as surface-renewal events.

Laboratory measurements show that the turbulent scalar flux at a hydrodynamically clean gas–liquid interface can be predicted by the surface-renewal approximation[7]

$$K \propto \left(\frac{D}{T}\right)^{1/2} \tag{1}$$

where K is the scalar transfer velocity, and T is the surface-renewal time scale or the reciprocal of the frequency of the appearance of the surface-renewal events, and D is the molecular viscosity of the scalar. The interactions of turbulent vortical structures with the free surface determine the frequency or the time scale. Therefore, understanding turbulence beneath the free surface is critical in evaluating the flux at the free surface. The hydrodynamically close relation between the vortical structures under the free surface and turbulence scalar transfer mechanisms has been determined by means of a direct numerical simulation (DNS) technique by Nagaosa,[4] Handler et al.,[5] and Nagaosa and Handler[6] at low Reynolds numbers. A typical example of such a direct relation between the near-wall vortical structures and the surface-renewal motions is found in Figures 22 and 23 in Nagaosa and Handler.[6] Details of vortical structures in the region adjacent to the free surface, their origin and time development, and the suitability of the surface-renewal approximation have also been elucidated by these numerical studies. The time scale of the surface-renewal events was not determined in these previous works because of limited information on the subsurface hydrodynamics.

An estimation of the characteristic time scale of the surface-renewal eddies is essential in establishing a predictive model for turbulent scalar transfer at a free surface. The variable-interval time-average (VITA) method has been applied to a time series of concentration signals of dye

Corresponding concerning the article should be addressed to R. Nagaosa at CEEE, University of Maryland, rnagaosa@umd.edu.

tracers measured in the region close to the free surface so as to evaluate the frequency of the surface-renewal in previous laboratory measurements.[1,2] This approach was designed to detect all the essential surface-renewal eddies in the vicinity of the free surface by optimizing several parameters, such as the time duration needed for time averaging and the threshold level needed to identify the surface-renewal eddies. Although these experiments have been successful in quantifying the surface-renewal frequency, optimization of several parameters has been found difficult to generalize for various kinds of turbulent flows. One of the reasons for this difficulty is attributed to the fact that previous laboratory experiments provided limited information on hydrodynamics in the subsurface region of turbulent open-channel flows. In particular, the entire details of three-dimensional (3-D) turbulent vortical structures in the turbulent flows with a free surface were not measured in laboratory experiments. Rashidi et al.[8] carried out laboratory experiments on turbulence measurements in open-channel flows to find the relation between the free-surface hydrodynamics and the turbulent scalar flux at the free surface based on a flow visualization technique. Rashidi[9] and Kumar et al.[10] applied their flow visualization techniques to observe the physical interactions of turbulent vortical structures with the free surface in turbulent open-channel flows. Pan and Banerjee[11] applied a DNS technique to a low-Reynolds number free-surface turbulence to determine the 3-D structure of vortices in the region very close to the free surface.

In the last decade, several studies have been carried out based on the latest experimental and numerical techniques to uncover the unresolved physics of turbulent scalar transport in the region very close to the interface. Magnaudet and Calmet [12,13] employed a large-eddy simulation (LES) technique to the turbulent open-channel flows of high Reynolds number $\mathrm{Re}_\tau = 1280$, with Schmidt numbers of $1 \leqq \mathrm{Sc} \leqq 200$. Here, $\mathrm{Re}_\tau = u_\tau\delta/\nu$ is the Reynolds number based on the wall-shear velocity, u_τ, water depth, δ, and kinematic viscosity of fluid, ν, and $\mathrm{Sc} = \nu/D$ is the Schmidt number. The Reynolds and Schmidt numbers that Magnaudet and Calmet considered in their LES are difficult to realize by a DNS technique. Therefore their work has revealed valuable information on the mechanisms of turbulent scalar exchange at large Reynolds and Schmidt numbers.

Herlina and Jirka[14] and Janzen et al.[15] conducted a series of laboratory experiments of turbulent scalar transport at a free surface based on the latest particle-image velocimetry (PIV) and laser induced fluorescence (LIF) techniques. They instrumented a grid-stirred tank with oxygen gas to measure the turbulent scalar flux and the subsurface velocity profiles simultaneously. Details of the turbulence statistics of velocity and oxygen-concentration fluctuations were obtained. The results of their laboratory experiments suggested that turbulent scalar transport at the free surface is governed by turbulent vortical structures with different length scales. They reported that the effect of the fine-scale turbulence is critical in determining the turbulent scalar flux at large Reynolds numbers, whereas large-scale turbulence plays an important role in determining turbulent scalar transfer mechanisms at low Reynolds numbers.

Kermani et al.[16] carried out a DNS of turbulent open-channel flows at Reynolds number $\mathrm{Re}_\tau \approx 300$. They investigated the effect of the Prandtl and Schmidt numbers on the turbulent heat and scalar transfer mechanisms for $\mathrm{Pr} = 0.71$, and $1 \leqq \mathrm{Sc} \leqq 8$, where Pr is the Prandtl number, which is defined by the ratio of fluid viscosity ν, and the thermal diffusivity of the fluid, α, $\mathrm{Pr} = \nu/\alpha$. They imposed both constant heat flux (the Neumann-type boundary condition) and constant concentration (the Direchlet-type boundary condition) conditions at the free surface. They also quantified the "surface age," which is equivalent to the mean residence time of fluid particles at the free surface, using Lagrangian tracing. They found that categorization of scalar transfer stages is possible using this approach.

Although such experimental and numerical investigations of turbulence and turbulent scalar transfer in the region close to the free surface have been carried out, no simple, predictive model for assessing the scalar flux has been proposed so far. In particular, the effect of the Reynolds number on turbulent scalar flux has not been given in these previous studies, except for our previous report.[6]

This study proposes a simple and predictive model for turbulent scalar transfer across a free surface. Here, we assume that the free surface is shear free and flat, which corresponds to the limit of zero Froude and Weber numbers. A DNS technique is employed for the purpose of obtaining information on the entire extent of the 3-D turbulence structures especially in the vicinity of the free surface. The Reynolds number is varied from $\mathrm{Re}_\tau = 150$ to 600 to examine the effect of the Reynolds number on the turbulent scalar flux and to compare the results from the present numerical predictions with those from laboratory experiments.[1,2] The Reynolds numbers in this study are $2300 < \mathrm{Re}_\mathrm{m} < 11{,}300$, where Re_m is the Reynolds number based on the bulk-mean velocity, U_m, and water height, δ, $\mathrm{Re}_\mathrm{m} = U_\mathrm{m}\delta/\nu$. These Reynolds numbers match those of the laboratory experiments performed by Komori et al.,[1,2] $2600 < \mathrm{Re}_\mathrm{m} < 12200$. Although several researchers have been interested in understanding the effect of the Schmidt (or Prandtl) number on turbulent scalar transfer at a free surface,[12,13,16,17] this study fixes the Schmidt number at 1 to determine the effect of the Reynolds number on transport. Scalings of turbulence statistics in this report use the wall-shear velocity, u_τ, water depth, δ, and fluid viscosity, ν, so as to ease comparisons of the results of this study with those obtained from laboratory experiments.[1,2] Although several reports on free-surface turbulence introduce other scalings of the turbulence statistics that do not rely on u_τ, and δ,[12,13,18,19] we will not attempt here to compare our results with them.

The concept of the surface-renewal approximation is introduced here to explore the physical relation between the free-surface hydrodynamics and turbulent scalar transfer across a free surface and to establish a predictive model for turbulent scalar flux. Two types of characteristic time scales of surface-renewal motions are proposed. One is the characteristic time scale derived from $T_\mathrm{S} = \Lambda/\mathscr{U}$, where Λ and $\mathscr{U}$ are the characteristic length and velocity scales, respectively. The other time scale is derived from the root-mean-square surface divergence, $T_\gamma = 1/\gamma_\mathrm{rms}$, where γ is the surface divergence, and subscript "rms" refers to its root-mean-square value. This time scale has been used by several researchers to model the turbulent scalar transfer at a free surface based on the subsurface hydrodynamics.[14,16,20–23] It is straightforward to correlate this time scale with turbulent scalar transport and the subsurface hydrodynamics, as the dimension of the surface divergence is the reciprocal of time, $[T]^{-1}$. It should also be emphasized here that measurements of γ in laboratory experiments are possible using the PIV technique.[14,15] In conclusion, it is the purpose of this

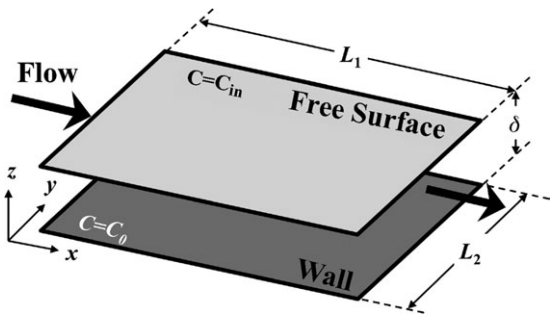

Figure 1. Flow configuration and coordinate system.

investigation to assess the suitability of the surface-renewal approximation using these two time scales.

Numerical Strategy

Assumptions at the free surface

We consider a fully developed turbulent water flow in an open channel. The free surface is assumed to be shear free and flat, corresponding to zero Froude and Weber numbers. This assumption has been justified in our previous laboratory experiments at low Reynolds numbers.[1–6] The Froude numbers in the laboratory experiments are $\mathrm{Fr}^2 = u_\tau^2/g\delta \approx O(10^{-3})$,[1,2] where u_τ is the friction velocity at the bottom wall, g is the gravitational acceleration, and δ is water height of the open channel. This Froude number range is considered small enough to ignore gravity-associated disturbances at the interface. Indeed, waves excited at the free surface observed in the laboratory experiments are too small to alter turbulence in the vicinity of the free surface significantly.

On the other hand, this assumption is not appropriate in turbulent flows with a thin water layer and a large mean velocity, (i.e., a turbulent liquid film), because the Froude number is relatively large in that case.[24] A typical example of the Froude number in turbulent liquid-film flows is $\mathrm{Fr}^2 = u_\tau^2/g\delta \approx O(10^{-1})$, with a water layer thickness of $\delta = 0.005$–0.01 m, and a mean velocity of $\mathrm{U_m} = 1$–4 m s^{-1}, resulting in a relatively large Reynolds number of $\mathrm{Re_m} = 12{,}000$–$33{,}000$. This situation is different from that of open-channel laboratory experiments, which have typical experimental conditions of $\delta = 0.01$–0.11 m, $U_\mathrm{m} = 0.06$–0.2 m s^{-1}, and $\mathrm{Re_m} = 2600$–12200.[1,2] It should be noted that the effect of the Froude number on free-surface hydrodynamics is rather limited regarding pressure–strain effects.[25] It is also true that significant differences between the laboratory experiments in which the Froude numbers are nonzero and numerical studies whose free surface is considered shear free have not been found in previous studies.[4–6] We conclude that the effect of the Froude number is not important for the purpose of exploring the free-surface hydrodynamics and associated turbulent scalar transfer mechanisms in the cases considered here.

Turbulent flow setup

Figure 1 shows the configuration of the turbulent open-channel flows used in this study. A fully developed turbulent flow is established between the bottom ($z = 0$) and at the gas–liquid interface ($z = \delta$). The main flow is in the x direction, driven by a well-controlled pressure gradient in the same direction, so as to maintain a constant wall-shear rate at the bottom. This flow is assumed to be periodic in the two interface-parallel directions, x and y. A stress-free boundary condition is adopted at the interface in accord with the assumption of a flat and shear-free interface. A no-slip boundary condition is used at the bottom of the open channel. Turbulent scalar transfer from the atmosphere to the bottom, across the free surface, is enforced by applying a constant concentration difference between the two interface-normal boundaries, $\Delta C = C_\mathrm{in} - C_0 \geq 0$, where C_in and C_0 are the concentrations at the free surface and the bottom, respectively. The concentration at the interface C_in and the bottom C_0 are assumed to be uniform in space and constant in time.

The fluid is assumed to be incompressible and Newtonian with constant density, ρ. A nondimensionalized version of the governing equations involves the conservation equations of mass, momentum and scalar, as follows

$$\frac{\partial}{\partial \overline{x_i}} u_i^+ = 0 \tag{2a}$$

$$\frac{\partial}{\partial \overline{t}} u_i^+ = -\frac{\partial}{\partial \overline{x_j}} u_j^+ u_i^+ + \frac{1}{\mathrm{Re}_\tau} \frac{\partial}{\partial \overline{x_j}} \frac{\partial}{\partial \overline{x_j}} u_i^+ - \frac{\partial}{\partial \overline{x_i}} p^+ \tag{2b}$$

$$\frac{\partial}{\partial \overline{t}} \overline{C} = -\frac{\partial}{\partial \overline{x_j}} u_j^+ \overline{C} + \frac{1}{\mathrm{Re}_\tau Sc} \frac{\partial}{\partial \overline{x_j}} \frac{\partial}{\partial \overline{x_j}} \overline{C} \tag{2c}$$

where t is time, u_i the velocity, p the pressure, and C the scalar concentration. The subscripts 1, 2, and 3 denote the streamwise (x), spanwise (y), and interface-normal (z) directions, respectively, and the summation convention is only applied to repeated alphabetic subscripts throughout this report. The parameters in Eqs. (2a)–(2c) are normalized as

$$u_i^+ = \frac{u_i}{u_\tau}, \quad p^+ = \frac{p}{\rho u_\tau^2}, \quad \overline{C} = \frac{C}{\Delta C}, \quad \overline{x_i} = \frac{x_i}{\delta}, \quad \overline{t} = \frac{t}{\delta/u_\tau} \tag{3}$$

The governing equations have two nondimensional parameters, Re_τ and Sc, as defined earlier.

Numerical strategies and flow parameterization

A DNS technique is used to solve the governing equations. The modified version of the numerical code used for computing turbulent flows at a stress-driven gas–liquid interface is applied here.[26] This numerical code uses a fractional step method proposed by Choi and Moin[27] for DNS of a turbulent channel flow. All the spatial derivatives are approximated by a second-order central difference scheme on a Cartesian staggered grid. A combination of a third-order Runge–Kutta method for nonlinear terms and a second-order Crank–Nicolson method for linear terms is used for integrating the governing equations in time. A direct solver for a Poisson-type partial differential equation based on fast Fourier transforms and Gaussian elimination is used to achieve high-computational performance.[28] A maximum residue of $|\partial u_i^+/\partial \overline{x_i}|$, which should be zero in an incompressible fluid, is about $\mathcal{O}(10^{-12})$ for $\mathrm{Re}_\tau = 150$ and $\mathcal{O}(10^{-11})$ for $\mathrm{Re}_\tau = 600$.

The details of the numerical setup are summarized in Table 1. Six runs of numerical simulations have been performed by varying the Reynolds number Re_τ between 150 and 600 with a fixed Schmidt number of $\mathrm{Sc} = 1$. Another Reynolds number, $\mathrm{Re_m}$, is used for the purpose of comparing the results from the present DNS with those obtained in previous laboratory experiments. The range of Reynolds numbers of $150 \leqq \mathrm{Re}_\tau \leqq 600$ corresponds to $2300 \lesssim \mathrm{Re_m} \lesssim 11{,}300$, which covers the range of Reynolds numbers obtained in the previous laboratory experiments by Komori

Table 1. Parameterization for the Present *In Silico* Experiments on Turbulent Flows with Scalar Transfer

Run	Re_τ	U_m	U_{surf}	Re_m	Sc	$ShSc^{-1/2}$	L_1/δ	L_2/δ	Grid Points	Δx^+	Δy^+	Δz^+	Δt^+_{ave}
I	150	15.3	18.1	2,300	1	4.67	5.0	2.50	256 × 288 × 97	9.20	4.09	0.183–3.49	0.385
II	180	15.7	18.7	2,840	1	5.49	4.0	2.00	256 × 288 × 109	8.84	3.93	0.174–3.83	0.353
III	240	16.4	19.1	3,950	1	7.03	3.0	1.50	256 × 288 × 137	8.84	3.93	0.169–4.14	0.301
IV	300	17.0	19.6	5,090	1	8.58	2.5	1.25	256 × 288 × 161	9.20	4.09	0.153–4.57	0.279
V	400	17.7	20.3	7,050	1	10.9	2.0	1.00	288 × 384 × 201	8.73	3.27	0.150–4.97	0.233
VI	600	18.7	21.2	11,300	1	15.5	2.0	1.00	432 × 512 × 271	8.73	3.68	0.135–5.79	0.175

The definitions of the notations are explained in the text.

et al.[1] Several numerical studies have supported the relation $K \propto Sc^{1/2}$ in turbulent flows with heat and scalar transfer.[12,13,16,17] Also, the surface-renewal approximation exhibits the same behavior, as explained later in this work. The effect of the Schmidt number on turbulent scalar transfer at a free surface is therefore not examined in this article.

The grid resolution used in all the numerical runs has been found to be fine enough to resolve all the essential scales of the turbulence. This has been confirmed by examining the fully developed turbulence statistics and the energy spectra of the velocity and scalar concentration fluctuations for Sc = 1. Our preliminary simulations find that increasing the Schmidt number from 1 to 2 results in an unphysical 3-D profile of the scalar concentration especially in the region close to the free surface. Therefore, given the grid resolution restriction in our DNS, Schmidt numbers are restricted to 1 or less. Sizes of the computational domain in both x and y directions, L_1 and L_2, are found to be large enough to obtain near-zero autocorrelations of velocities and concentration for the maximum separations, $L_1/2$ and $L_2/2$. The computational lengths in the interface-parallel directions are the same, or larger than those of Moser et al.,[29] $L_1/\delta_c = 4.0$ and $L_2/\delta_c = 2.0$ for $Re_\tau \approx 180$ and $L_1/\delta_c = 2.0$ and $L_2/\delta_c = 1.0$ for $Re_\tau \approx 400$ and 600, where δ_c here is the half-width of the two-dimensional (2-D) channel. The time increment for integration of the governing equations is determined dynamically to keep the Courant number around $\sqrt{3}$ in every numerical run. The average time step, $\Delta t^+_{ave} = \Delta\langle tu_\tau^2/\nu\rangle$, is about 0.38 at $Re_\tau = 150$ and 0.17 at $Re_\tau = 600$. Statistically reliable turbulence statistics are computed from a series of instantaneous turbulent flow realizations, which cover more than 4500 viscous wall units. The DNS database established by Moser et al.[29] has been used to verify the accuracy of these turbulence statistics obtained by the present DNS. Several comparisons between the present DNS and those computed by Moser et al.[29] reveal that the present simulations represent physically accurate 3-D turbulence. The results of the comparisons are shown in the next section.

Surface-renewal approximation

The turbulent scalar flux at the interface, Q, can be estimated using the scalar transfer velocity, K, as

$$Q = K \cdot \Delta C \tag{4}$$

where ΔC is the concentration difference between the wall and the free surface, $\Delta C = C_{in} - C_0$. The surface-renewal approximation was introduced originally by Dankwerts to predict the scalar transfer velocity, K, theoretically.[7] In this approximation, K is expressed by Eq. 1, that is $K = a\,(D/T)^{1/2}$. This approximation involves a constant of proportionality, a, which should be determined by an appropriate method. The original derivation of the surface-renewal approximation implies $a = 1$ by assuming random and continuous replacement of fluid at the free surface with a constant replacement rate. This situation is not likely to be realized, as the replacement of fluid elements at the free surface will be random but intermittent. Determination of the constant a based on the experiments or numerical simulations is critical in developing a predictive model for turbulence scalar flux between the atmosphere and the turbulent water. Therefore the goal of this study is to determine the proportionality constant, a, using results of our DNS.

The following relation can be derived from Eq. 4 and Fick's law of diffusion, $Q = D\,(\partial C/\partial x_3)_{x_3 = \delta}$

$$K = \frac{D}{\Delta C}\left(\frac{\partial C}{\partial x_3}\right)_{x_3=\delta} \tag{5}$$

The time-space average of the scalar transfer velocity, $\langle K\rangle$, is expressed using Eq. 5 as

$$Sh = \frac{\langle K\rangle\delta}{D} = \left(\frac{\partial\langle\overline{C}\rangle}{\partial\overline{x_3}}\right)_{x_3=\delta} \tag{6}$$

where $Sh = \langle K\rangle\delta/D$ is the Sherwood number, and $\langle.\rangle$ denotes time-space averaging over x, y, and t. In Kermani et al.,[16] a different definition of the scalar transfer velocity is used

$$Q = K_0 \cdot \delta C \tag{7}$$

where $\delta C \equiv C_{in} - C|_{z=\delta/2}$, and $C|_{z=\delta/2}$ is the time-space average of the concentration of scalar at the center of the open channel, $z = \delta/2$. It is obvious that the two scalar transfer velocities can be related by $K = K_0(\delta C/\Delta C)$.

The surface-renewal approximation, Eq. (4), can be normalized as

$$Sh\,Sc^{-1/2} = a\,Re_\tau\langle T^+\rangle^{-1/2} \tag{8}$$

or

$$\langle K^+\rangle Sc^{1/2} = a\langle T^+\rangle^{-1/2} \tag{9}$$

where $K^+ = K/u_\tau$ and $T^+ = T/(\nu/u_\tau^2)$ are the nondimensional scalar transfer velocities and the characteristic time scale, respectively. It is also clear that the two normalized scalar transfer velocities are related by $\langle K^+\rangle = ShSc^{-1}Re_\tau^{-1}$.

Eqs. 8 and 9 reveal that the Sherwood number is proportional to the square root of the Schmidt number, $Sh \propto Sc^{1/2}$. The suitability of this relation has been confirmed by several numerical studies by LES[12,13,17] and DNS.[16] For this reason, this work focuses on investigations of the effect of the Reynolds numbers on the turbulent scalar flux at a free surface, rather than pursuing Schmidt number effects.

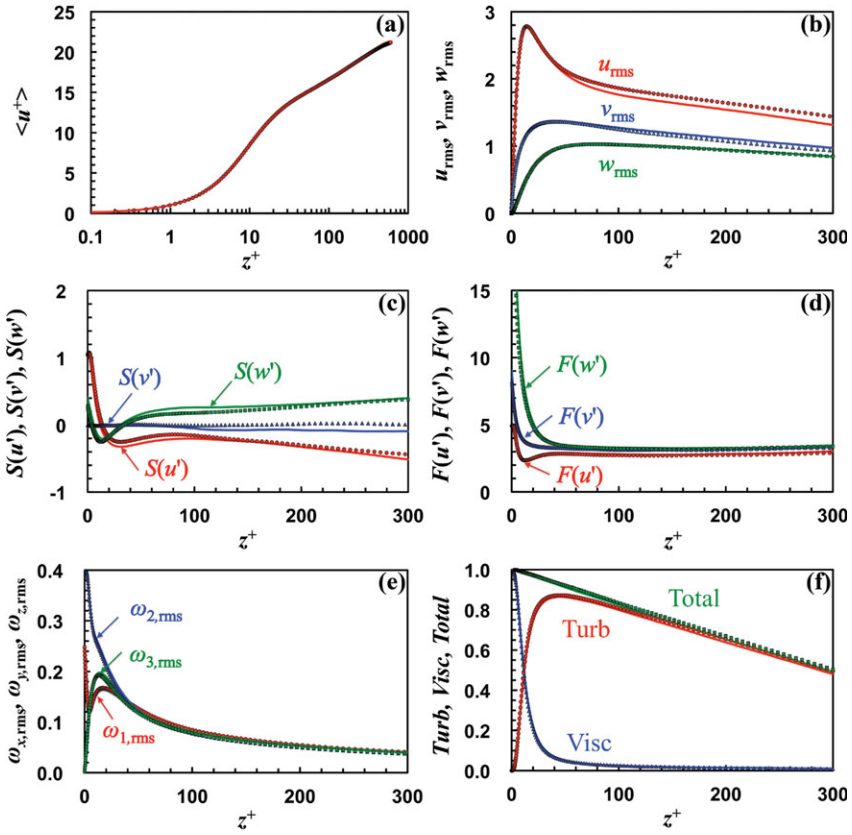

Figure 2. Fully developed turbulence statistics at $Re_\tau = 600$ at the near-wall region of $0 \leq z^+ \leq 300$ for comparisons of this study and those obtained by Moser et al.[29] in the 2-D closed channel.

Each plot indicates (a) mean velocity; (b) root-mean-square velocity fluctuations; (c) skewness of velocity fluctuations; (d) flatness of velocity fluctuations; (e) root-mean-square vorticity fluctuations; and (f) the Reynolds, viscous, and total stresses. Lines and symbols in plots (a)–(f) denote the results of Moser et al.,[29] and the present numerical simulation, respectively. [Color figure can be viewed in the online issue, which is available at wileyonlinelibrary.com.]

Results

Fully developed turbulence statistics

We now confirm the accuracy of the present results by comparing them with those obtained by Moser et al.[29] In particular, we focus on the results of $Re_\tau = 600$, the largest Reynolds number case, and Moset et al.'s DNS database of $Re_\tau \approx 600$ for turbulent 2-D channel flow.

We first define certain quantities and relations that are used in this comparison in Figure 2. The root-mean-square, skewness, and flatness of the turbulent quantity h are defined as follows

$$h_{rms} = \langle h'^2 \rangle^{1/2} \tag{10a}$$

$$S(h') = \langle h'^3 \rangle / h_{rms}^3 \tag{10b}$$

$$F(h') = \langle h'^4 \rangle / h_{rms}^4 \tag{10c}$$

where h' signifies the fluctuation around its time-space average, $\langle h \rangle$. Inserting $u_i = \langle u_i \rangle + u_i'$ $(i = 1\text{–}3)$, $\langle u_2 \rangle = \langle u_3 \rangle = 0$, and $p = \langle p \rangle + p'$ into Eq. 2b and taking its time-space average, we obtain the following equation, which shows the relation between the Reynolds and viscous shear stresses

$$\underbrace{-\langle w'^+ u'^+ \rangle}_{\text{Turb}} + \underbrace{\frac{1}{Re_\tau}\left(\frac{\partial \langle u^+ \rangle}{\partial \bar{z}}\right)}_{\text{Visc}} = \underbrace{1 - \frac{z^+}{Re_\tau}}_{\text{Total}} \tag{11}$$

Also, the vorticity, ω_i, is defined by

$$\omega_i = \varepsilon_{ijk} \frac{\partial u_j}{\partial x_k} \tag{12}$$

where ε_{ijk} is the Eddington's alternating tensor.

The comparison shown in Figure 2 is given in the region of the lower half of the open-channel $(0 \leqq z^+ \leqq 300)$, as the effect of the free surface on turbulence statistics is significant in the upper 1/3 of the domain, that is, $400 \leqq z^+ \leqq 600$. This figure shows that the results of the present numerical simulations agree well with those of Moser et al.,[29] who used a pseudospectral method for solving the governing equations. It should be noted here that the skewness and flatness of the velocity fluctuations and the root-mean-square vorticity fluctuations are affected strongly by the fine-scale turbulence fluctuations. Excellent agreements in plots (c)–(e) in Figure 2 is therefore good evidence that the present numerical simulations represent the fine-scale turbulence in the open channel in a satisfactory manner.

Later in this work, the energy spectra of u_3' in the region very close to the free surface is used to evaluate the characteristic length scale of the surface-renewal motions. Thus, the adequacy of the energy spectra given by the present DNS should be assessed, as turbulent fluctuations in a DNS database obtained by a finite difference method are considered to be affected by numerical dissipation particularly at high wavenumber scape. The DNS database of Moser et al.[29] is also

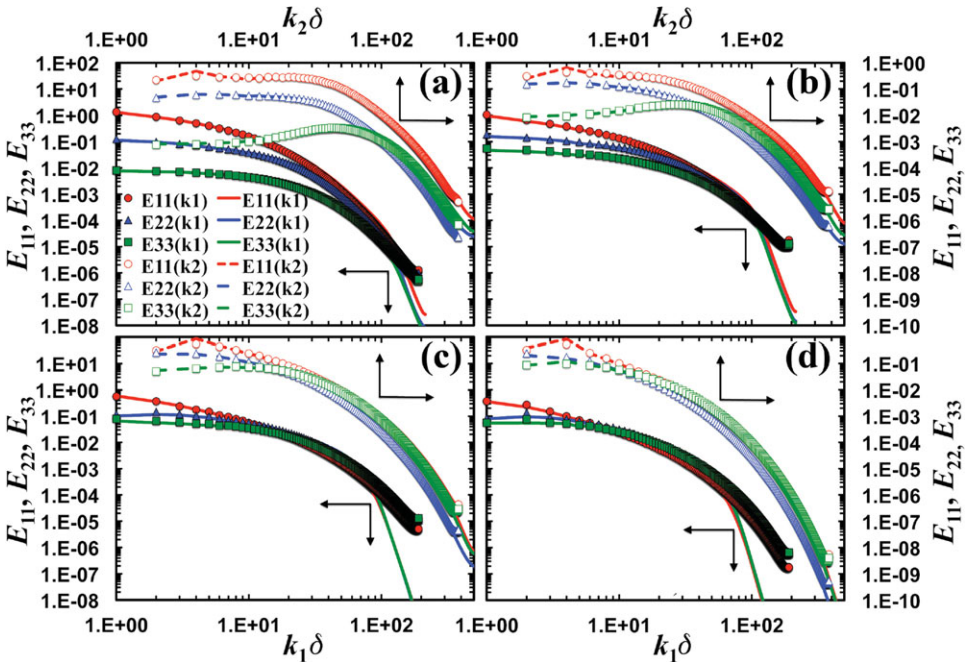

Figure 3. Comparisons of energy density spectra at $Re_\tau = 600$: (a) $z^+ \approx 10$; (b) $z^+ \approx 30$; (c) $z^+ \approx 100$; and (d) $z^+ \approx 300$.

Lines and symbols indicate the results from the present DNS and those by Moser et al.,[29] respectively. [Color figure can be viewed in the online issue, which is available at wileyonlinelibrary.com.]

used here to verify the soundness of the energy spectra computed from the present numerical simulations.

Figure 3 shows comparisons of the energy density spectra in the case of $Re_\tau = 600$. The energy density spectra is defined by

$$E_{\alpha\alpha}(k_\beta\delta) = \frac{1}{2\pi}\left\langle \mathcal{F}_\beta(u'_\alpha)\mathcal{F}^*_\beta(u'_\alpha)\right\rangle, \quad (\alpha = 1,2,3; \quad \beta = 1,2) \tag{13}$$

where $\mathcal{F}(u'_\alpha)$ signifies the Fourier transform of u'_α in the β-th direction, and * denotes the complex conjugation. The present simulations are seen to agree well with Moser et al.,[29] especially at low wavenumbers. At high wavenumbers, we observe a rapid decay of the energy spectra $E_{\alpha\alpha}(k_1\delta)$ (α = 1–3) as the wavenumber k_1 increases, particularly at $z^+ \approx 100$ and 300. The effect of this decay is negligible, as the decay occurs only at very fine scales, for example, $k_1\delta > 100$ at $z^+ \approx 100$ and $k_1\,\delta > 70$ at $z^+ \approx 300$, corresponding to a length scale of about $4\Delta x^+$, and $6\Delta x^+$, respectively. We have also confirmed that similar excellent agreement exists between the present DNS and those in the database of Moser et al.[29] for $Re_\tau = 180$ and 400.

Turbulent scalar flux at a free surface

In the previous section, fully developed turbulence statistics obtained by the present DNS are compared with those of Moser et al.[29] The comparison shows clearly that the present numerical predictions provide very exact turbulent flow realizations of open-channel flows at the given Reynolds numbers. It is also worth comparing the turbulent scalar flux at the free surface obtained from the present predictions with those measured experimentally by Komori et al.[1,2]

The authors already attempted a comparison of the Sherwood numbers obtained by the DNS technique with those measured by laboratory experiments at two Reynolds numbers, $Re_\tau = 150$ and 300.[6] It was found that the numerically predicted Sherwood numbers agree well with those obtained by the laboratory experiments, although the effect of the Reynolds number on the turbulent scalar flux could not be determined because of limited numerical data. Here, we extend the previous comparison between the laboratory and numerical experiments by providing additional numerical predictions of the Sherwood numbers at larger Reynolds numbers. As stated earlier in this article, the Reynolds numbers covered by the present numerical simulations, $150 \leqq Re_\tau \leqq 600$ or $2300 \lesssim Re_m \lesssim 11{,}300$, are comparable with those of the laboratory experiments of Komori et al.,[1,2] whereas the Schmidt numbers in the present DNS (Sc = 1) and the laboratory experiments (Sc $\approx$ 600) are different. Several numerical studies on turbulent scalar transfer at a free surface have indicated that the scalar transfer velocity is proportional to $Sc^{1/2}$.[2,12,13,16,17] It should be stressed here that the relation of $Sh \propto Sc^{1/2}$ does not guarantee that physical mechanisms of turbulent scalar transfer are the same at low and high Sc.

Figure 4 compares the scalar transfer velocity obtained in the present numerical simulations with those obtained in the experiments. We obtain $ShSc^{-1/2} = 4.67$ at $Re_\tau = 150$ and $ShSc^{-1/2} = 8.58$ at $Re_\tau = 300$ from the present simulations. These predictions agree well with those Nagaosa and Handler[6] already reported, $ShSc^{-1/2} = 4.77$ at $Re_\tau = 150$ and $ShSc^{-1/2} = 8.63$ at $Re_\tau = 300$. Kermani et al.[16] also predicted the turbulent scalar flux at the free surface and proposed $\langle K_0^+\rangle = 0.611\ Sc^{-0.456}$ at $Re_\tau = 300$. This correlation relation gives $\langle K_0^+\rangle = 0.0611$ at Sc = 1, resulting $\langle K^+\rangle \approx 0.0281$, or, $ShSc^{-1/2} \approx 8.43$, as $\delta C/\Delta C \approx 0.46$ is obtained from Figure 2b in Kermani et al.[16] Therefore, the results of Kermani et al. also agree well with our results.

Comparisons between the results of the present DNS and those measured by Komori et al.[1,2] in Figure 4 find that our present predictions of scalar flux agree with those of the laboratory experiments, especially in the region of low Reynolds numbers, that is, $Re_m \leqq 7000$ ($Re_\tau \leqq 400$). The results of the present predictions show that $ShSc^{-1/2}$ obtained by the present DNS is proportional to $Re_m^{3/4}$, whereas the laboratory

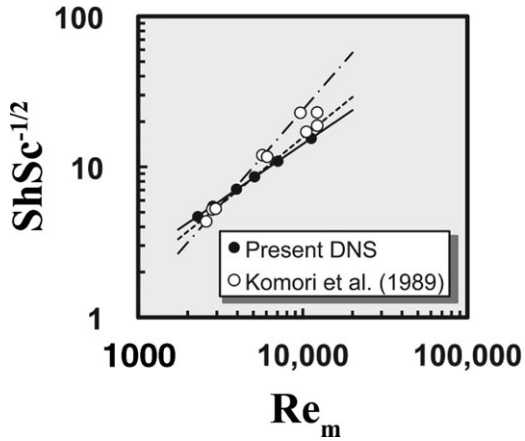

Figure 4. The effect of the Reynolds number Re_m on the Sherwood number Sh.

The results of the present DNS and the laboratory experiments[1,2] are plotted by closed and open circles, respectively. The solid line shows, $ShSc^{-1/2} \propto Re_m^{3/4}$, which is the best-fit result of the present DNS. The dashed and chain-dotted lines indicate the lowest and highest cases of the best-fit results of the experimental results by Komori et al.,[1,2] respectively.

measurements show $ShSc \propto Re_m^n$, where $0.89 < n < 1.26$. A quantitative comparison between the results from the present DNS and the laboratory measurements by Komori et al.[1,2] is difficult, as the results of the laboratory measurements exhibit considerable scatter. It is nevertheless clear from this comparison that the present DNS provides acceptable prediction of the Sherwood numbers, which are underestimated at the Reynolds number $Re_\tau \geq 400$ or $Re_m \sim 7000$. The present DNS ignores the effect of surface disturbances due to surface waves because of our assumption of zero Weber and Froude numbers. Incorporation of the Weber and Froude numbers should improve the accuracy the prediction of $ShSc^{-1/2}$, as attempted by Tamburrino and Gulliver.[20]

It is reasonable to conclude that the present numerical simulations predict turbulent scalar fluxes at a free surface within acceptable margin of errors in the Reynolds number covered here. It is also expected that the mechanisms of turbulent scalar transfer can be understood in detail using the present turbulent flow realizations.

Free-surface hydrodynamics

Figure 5 depicts a 3-D view of turbulent vortical structures and low-concentration regions, $\overline{C} < -C_{rms,max}$, for $Re_\tau = 600$, where $C_{rms,max}$ is the local maximum value of C_{rms} in the region near the free surface, $C_{rms,max} \approx 0.136$ at $z^+ \approx 583$ ($\overline{z} \approx 0.97$). 3-D turbulent vortical structures are extracted using the Laplacian of the pressure

$$Q \equiv \frac{\partial}{\partial x_i}\frac{\partial}{\partial x_i}p = \frac{1}{2}\left(\Omega^2 - \mathbf{S}^2\right) \tag{14}$$

where $\mathbf{S}^2 = \mathbf{S}^t\mathbf{S}$ and $\Omega^2 = \Omega^t\Omega$, with $\mathbf{S}$ and Ω are the symmetric and antisymmetric parts of the velocity gradient tensor, respectively. Vortical structures in Figure 5 are identified by $\hat{Q} = (Q - \langle Q \rangle)/Q_{rms} \geq 3/2$.[6] Emerging low-concentration fluid in the region near the free surface indicates that the turbulent scalar flux is boosted there by intensifying the concentration gradient, $(\partial C'/\partial z)_{z=\delta}$. This figure indicates that interactions of vortical structures with the free surface is associated with low-concentration fluid by being transported from the turbulent bulk, as illustrated in our previous study.[4] Obtaining the characteristic time scale associated with these surface-renewal motions is a major goal of this work.

Several researchers[14,15,20,21,30,31] have already focused attention on using the surface divergence to model turbulent scalar flux at the free surface. The surface divergence, γ, is defined as

$$\gamma(x_1, x_2, t) \equiv \left(\frac{\partial u_1'}{\partial x_1} + \frac{\partial u_2'}{\partial x_2}\right)_{x_3=\delta} = -\left(\frac{\partial u_3'}{\partial x_3}\right)_{x_3=\delta} = -\left(\frac{u_3'|_{x_3=\delta} - u_3'|_{x_3=\delta-\Delta\delta}}{\Delta\delta}\right) \tag{15}$$

where $\Delta\delta$ is the distance between the free surface and the first mesh point below the free surface. It is obvious that $u_3'|_{x_3=\delta}$ in Eq. 15 should be zero because of the boundary condition at the free surface. Therefore Eq. 15 leads to $\gamma(x_1, x_2, t) = u_3'|_{x_3=\delta-\Delta\delta}/\Delta\delta$. It is clear from this that positive surface divergence is produced by turbulent impingement from turbulent bulk toward the free surface, $u_3'|_{x_3=\delta-\Delta\delta} > 0$, and negative surface divergence, on the other hand, is associated with a downdraft, $u_3'|_{x_3=\delta-\Delta\delta} < 0$.

Figures 6a,b show a comparison of instantaneous distributions of the surface divergence and the subsurface concentration fluctuation at one grid point below the free surface for $Re_\tau = 600$ ($\Delta\delta^+ \approx 0.135$). A comparison between Figures 6a,b also indicates that the positive (negative) surface divergence is found at locations where negative (positive) concentration fluctuations are established. This comparison suggests that the positive surface divergence, which is characterized by the diverged velocity vectors, strengthens turbulent scalar flux locally. This hydrodynamic phenomenology is easily explained by the fact that the upward currents from turbulent bulk toward the free surface bring low-concentration fluid in the vicinity of the free surface and that the thickness of the turbulent boundary layer adjacent to the free surface is reduced by such fluid motions. Consequently, the turbulent scalar flux increases locally there. In addition to that, the two plane distributions of the surface divergence and the concentration fluctuation are observed to be very similar, suggesting that the correlation coefficient between the surface divergence and the local scalar gradient perpendicular to the free surface, $G = (\partial C'/\partial z)_{z=\delta}$, will be large enough.

The statistical relation between the surface divergence and the local scalar flux, $G = (\partial C'/\partial z)_{z=\delta}$ should be examined to

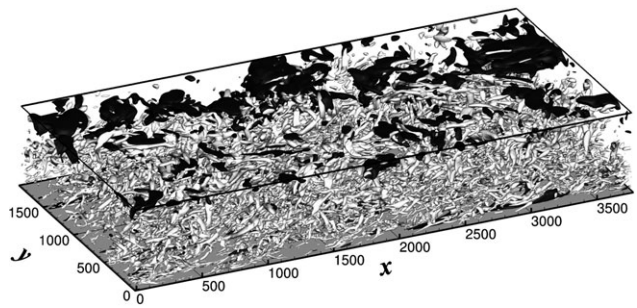

Figure 5. 3-D view of turbulent vortical structures for $Re_\tau = 600$, with low-concentration regions $\overline{C} < -C_{rms,max}$.

These vortical structures, indicated by surfaces with light-gray, are extracted by $\hat{Q} \geq 3/2$. Low-concentration fluid with the threshold of $C_{rms,max} \approx 0.14$, is signified by dark-gray contour surfaces.

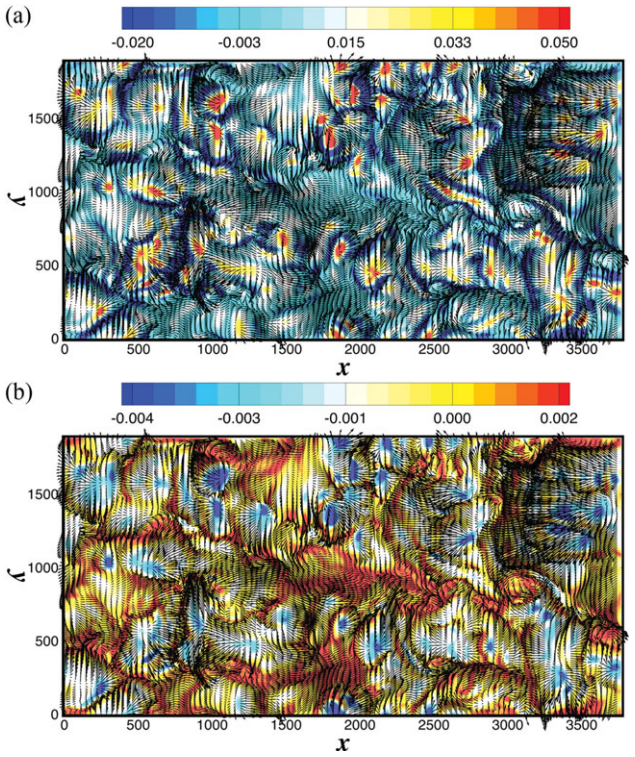

Figure 6. Free-surface hydrodynamics in the case of Re_τ = 600; (a) 2-D distribution of the surface divergence; and (b) 2-D distribution of the concentration fluctuation at one mesh point below the free surface ($z^+ \approx 599.87$).

The velocity vectors are mapped at every four grid points at the free surface. Both the surface divergence and the concentration fluctuation are normalized as $\gamma^+ = (\nu/u_\tau^2)\ \gamma$ and $\overline{C'} = C'/\Delta C$, respectively. [Color figure can be viewed in the online issue, which is available at wileyonlinelibrary.com.]

assess their similarity. The correlation coefficient between the surface divergence and local turbulent scalar flux is expressed by

$$R_{\gamma G} = \frac{\langle \gamma(x_1, x_2, t) G(x_1, x_2, t) \rangle}{\gamma_{\rm rms} G_{\rm rms}} \tag{16}$$

Figure 7 shows the effect of the Reynolds number Re_τ on the correlation coefficient $R_{\gamma G}$. The correlation coefficient increases slightly with increasing Reynolds number and approaches 0.75 for $Re_\tau \geq 300$. It is therefore reasonable to consider the surface divergence to establish a predictive model for turbulent scalar transfer. One of the advantages in introducing the surface divergence is that the surface divergence can be measured using the latest experimental techniques such as PIV.[14,15,20,21] The concentration gradients of the scalar at the free surface, in contrast, are difficult to measure in the laboratory, because this requires very exact measurements of the local concentration in the very thin turbulent boundary layers below the free surface. Indeed, only a few reports on the direct measurement of the scalar concentration gradient in the region below a free surface have been published so far, for example, Harlina and Jirka,[14,32] and Janzen et al.,[15] which use PIV-LIF techniques to measure concentration fluctuation near the free surface.

Characteristic time scales at a free surface

Here, we investigate the two characteristic time scales mentioned previously. One is a time scale based on the characteristic length and velocity scales, $T_S = \Lambda/\mathscr{U}$. The other is defined by the reciprocal of the root-mean-square surface divergence, $T_\gamma = 1/\gamma_{\rm rms}$.

The free-surface hydrodynamics depicted in Figure 6a suggests that many patch-like patterns, which are signified by positive surface divergence, cover the whole of the free surface. It is also evident from the comparison of Figures 6a,b that these patch-like structures are "foot prints" of the interactions of the turbulence with the free surface, which strengthen turbulent scalar transport. In this study, the autocorrelation coefficient of the surface divergence in the streamwise direction given by

$$C_{\gamma\gamma}(r_1) = \frac{\langle \gamma(x_1 + r_1, x_2, t)\gamma(x_1, x_2, t) \rangle}{\gamma_{\rm rms}^2} \tag{17}$$

is used to evaluate the characteristic length scale of these patch-like structures.[33] The autocorrelation coefficient is computed from the energy density spectra of u_3' at one computational mesh below the free surface, $z = \delta - \Delta\delta$, using the Weiner–Khinchine theorem.[34] The distributions of the power spectra of the surface divergence in the streamwise direction, $E_{\gamma\gamma}(k_1\delta) \equiv \langle \mathscr{F}(\gamma)\mathscr{F}^*(\gamma) \rangle / (2\pi) = (1/\Delta\delta)^2\, E_{33}(k_1\delta)|_{z=\delta-\Delta\delta}$, and autocorrelation coefficients, $C_{\gamma\gamma}(r_1)$, for six numerical runs are shown in Figure 8. $E_{\gamma\gamma}(k_1\delta)$ is normalized to satisfy $\int dk_1 E_{\gamma\gamma} = 1$ in this figure. The profiles of the autocorrelation coefficients indicate clearly that the zero-correlation length scale, $C_{\gamma\gamma}(\lambda) = 0$, exists in all numerical runs in the region $0 < r_1^+ < 150$. This length scale can be thought of the "radius" of the patch-like patterns. Therefore, double the length of scale λ corresponds to the characteristic length scale of the patch-like structures, that is, $\Lambda = 2\lambda$ is associated with positive surface divergence $\gamma > 0$ at the free surface.

The effect of the Reynolds number Re_m on the characteristic length scale, $\overline{\Lambda} = \Lambda/\delta$, is shown in Figure 9. The results of the present DNS indicate that the nondimensionalized length scale is proportional to $Re_m^{-1/2}$. The laboratory experiments by Komori et al.,[2] did not find a clear relationship between the Reynolds number and the length scale, and the authors conclude that the length scales are in the range $0.37 < \overline{\Lambda} < 1.1$ at the Reynolds numbers they examined, 2600 <

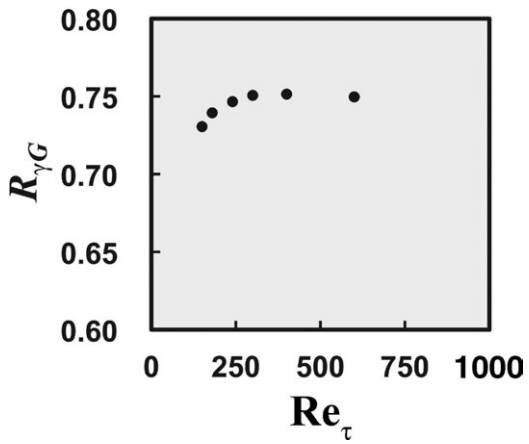

Figure 7. The effect of the Reynolds number on the correlation coefficient, $R_{\gamma G}$.

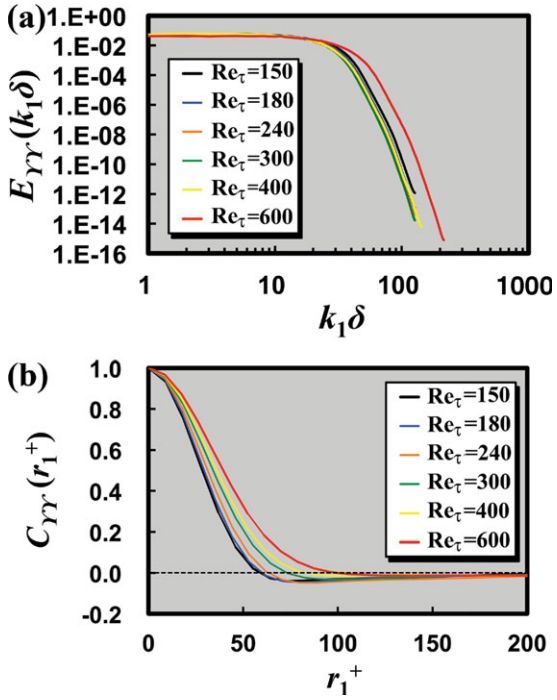

Figure 8. (a) Power spectra of the surface divergence; and (b) the distributions of the autocorrelation coefficients in the streamwise direction.

Power spectra shown in (a) are normalized to satisfy $\int dk_1\ E_\gamma = 1$. [Color figure can be viewed in the online issue, which is available at wileyonlinelibrary.com.]

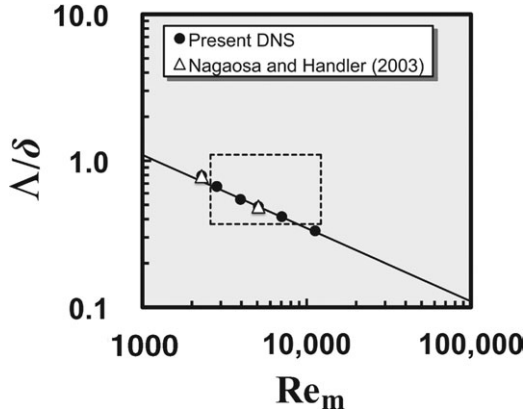

Figure 9. The effect of the Reynolds number Re$_m$ on the characteristic length scale at the free surface.

The characteristic length scale is normalized by water depth, δ. The solid line indicates the best-fit result for the present DNS data for the data Re$_\tau \geq$ 240, $\overline{\Lambda} \propto$ Re$_m^{-1/2}$. The hatched gray region indicated by a dashed line covers the results of the laboratory experiments by Komori et al.,[2] 0.37 $< \overline{\Lambda} <$ 1.1 at 2600 $<$ Re$_m <$ 12,200. Open triangles indicate the results of Nagaosa and Handler.[6]

Re$_m$ $<$ 12,200, as indicated by the dotted region in this figure. These results suggest that the present evaluations of the characteristic length scales appear to be acceptable considering the fact that they are of the same order of magnitude as those measured by Komori et al.[2]

Our previous analysis of the characteristic length scales of 3-D vortical structures in the region adjacent to the free surface revealed that $\overline{\ell} = \ell/\delta = 0.785$ at Re$_\tau$ = 150 (Re$_m$ = 2300), and $\overline{\ell} = 0.524$ at Re$_\tau$ = 300 (Re$_m$ = 5110), where ℓ is the length scale of the turbulence structures in the streamwise direction in the subsurface region evaluated by the spatial two-point correlations of the vorticity field.[6] These values are very close to the results of the present analysis based on the autocorrelation coefficient of the surface divergence, $\overline{\Lambda} = 0.790$ for Re$_\tau$ = 150, and $\overline{\Lambda} = 0.487$ for Re$_\tau$ = 300, as plotted by open triangles in Figure 9.

The characteristic velocity scale for turbulent scalar transport is estimated by the horizontal root-mean-square velocity fluctuation at the free surface (see Janzen et al. [15]). Hence, the characteristic velocity scale is estimated by $\mathscr{U} = (u_{rms}^2 + v_{rms}^2)^{1/2}$. The velocity scales appear to be constant at $\mathscr{U} \equiv \mathscr{U}/u_\tau \approx 1.2$ for the Reynolds numbers covered in this work. The characteristic time scale for surface-renewal events is consequently given by $T_S = \Lambda/\mathscr{U}$.

The relation between the characteristic time scales, T_S and T_γ, and the Reynolds number Re$_m$ is shown in Figure 10. The results of the laboratory experiments of the characteristic time scale measured by Komori et al.[1] are also plotted in the same figure by open circles. Komori et al.[1] measured the surface-renewal frequency f using a time series of concentration signals of a dye tracer released from inside the turbulent boundary layer, and the time scale is obtained by $T = 1/f$. All the time scales here are normalized as $\overline{T} = T/(\delta/u_\tau)$ to compare the results of this study with those measured by the previous laboratory experiments. The present numerical simulations show that the two characteristic time scales, $\overline{T_S}$, and $\overline{T_\gamma}$, are proportional to Re$_m^{-3/5}$. In contrast, the laboratory experiments by Komori et al.[1] suggest a different relation between Re$_m$ and the characteristic time scale, that is, $\overline{T} \propto$ Re$_m^{-1}$. It should be mentioned here that the characteristic time scales $\overline{T_S}$ found in the present DNS are close to those measured by Komori et al. at 2300 $<$ Re$_m <$ 7000. The discrepancy between $\overline{T_S}$ and the laboratory experiments widens, as the Reynolds number increases.

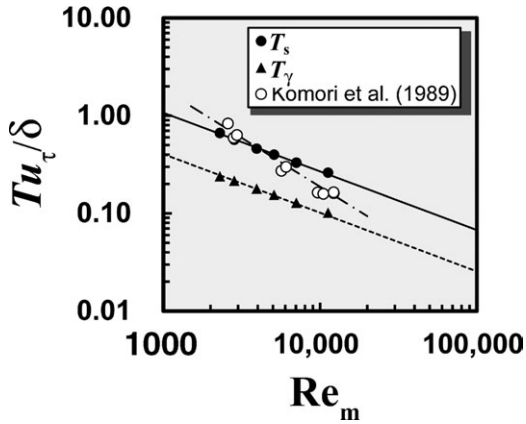

Figure 10. The characteristic time scale at the free surface.

The solid and open plots are the results of the present DNS and those by the laboratory experiments by Komori et al.[1] Both the solid and the dashed lines indicate the best-fit results for $\overline{T_S}$, and $\overline{T_\gamma}$, respectively. Both the time scales predicted by the present DNS are proportional to Re$_m^{-3/5}$, as indicated by both the solid and the dashed lines. The results of the laboratory experiments, on the other hand, reveal that the time scale is proportional to Re$_m^{-1}$, as shown by the chain-dotted line.

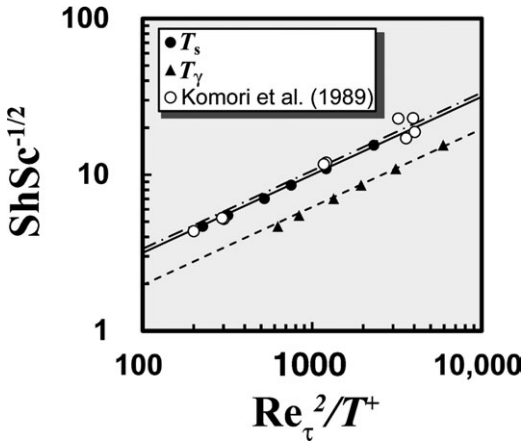

Figure 11. The relation between Re_τ^2/T^+ and $ShSc^{-1/2}$ for the present numerical simulations and the laboratory experiments by Komori et al.[1]

The two characteristic time scales T_S and T_γ are verified to discuss suitability of the surface-renewal approximation. The solid and dashed lines indicate the best-fit results for T_S and T_γ, respectively. The chain line is the relation $ShSc^{-1/2} = aRe_\tau(T^+)^{-1/2}$ with $a \approx 0.34$, as observed by Komori et al.[1]

Proper time scale for predicting turbulent scalar flux

The suitability of the two characteristic time scales, T_S, and T_γ, for predicting turbulent scalar transport at a free surface is assessed based on the nondimensional version of the surface-renewal approximation expressed by Eq. 8. Figure 11 shows the relation between Re_τ^2/T^+ and $ShSc^{-1/2}$ for the two characteristic time scales, T_S^+, and T_γ^+. For quantitative comparison, the results of laboratory experiments[1] are also indicated by open circles in the same figure. The two characteristic time scales are found to be suitable, as each satisfies the relation $ShSc^{-1/2} \propto Re_\tau/(T^+)^{1/2}$. The constant of proportionality a in Eq. 8 is 0.32 for T_S and 0.20 for T_γ in the present DNS, whereas Komori et al. [1,2] found experimentally that the constant is approximately 0.34 for turbulent open-channel flows. It should be pointed out that the time scale T_S appears to be very similar to the time scale measured by Komori et al.[1,2] On the other hand, T_γ will be different from the time scale determined in the laboratory experiments, although it also satisfies the surface-renewal approximation.

Kermani et al.[16] reported that the scalar transfer velocity is estimated by $\langle K_0^+ \rangle\ Sc^{1/2} = A\gamma_{rms}^{1/2}$, with the constant of proportionality of $0.41 < A < 0.45$ for $1 \leqq Sc \leqq 8$. The range of the constant corresponds to $0.19 \lesssim a \lesssim 0.21$, using the relation $a = A\ (\delta C/\Delta C)$, and $\delta C \approx 0.46$. This result shows excellent agreement with our result, $a = 0.20$. The correlation relation that we propose in this work, $ShSc^{-1/2} = a(Re_\tau^2/T_\gamma)^2$ with $a = 0.20$, is therefore appropriate for evaluating the turbulent scalar flux. Law and Khoo,[35] Tamburrino and Gulliver,[20] McKenna and McGillis,[21] Magnaudet and Calmet,[13] Hasegawa and Kasagi,[23] and Janzen et al.[15] proposed their own correlation between the scalar transfer velocity and the surface divergence. However, quantitative comparisons of those results with the results of this study are difficult, because the flow setup and scaling of the hydrodynamics parameters are different in those studies.

In conclusion, the characteristic time scale T_S discussed in this study is essentially equivalent to that measured by the laboratory experiments using dye tracer concentration signals with the aid of the VITA technique. In contrast, the characteristic time scale T_γ seems to be different from T_S obtained in laboratory experiments. It is interesting that the ratio between T_S and T_γ is approximately 2.6 at the Reynolds numbers that we deal with in this study. This fact suggests that some physical relation between the two time scales could be extracted by a proper scaling analysis.

Conclusions and Future Directions

Conclusions

This study investigates the characteristic time scale for predicting turbulent scalar flux based on the physical mechanisms of the transport phenomena in the vicinity of a free surface. The surface-renewal approximation is implemented to correlate the free-surface hydrodynamics and turbulent scalar flux. A DNS is used here to obtain 3-D details of turbulence in open-channel flows, especially in the region very close to the free surface, and also to obtain turbulent scalar transfer rates across the free surface. Here, we propose the use of two characteristic surface-renewal time scales to evaluate the turbulent scalar flux at the free surface. It was determined, using the surface-renewal approximation, that the proportionality constants are 0.32 for T_S and 0.20 for T_γ. The constant 0.32 for T_S is very close to the constant observed in the laboratory experiments of Komori et al., 0.34.[1,2] Hence, the characteristic time scale T_S defined in this study is essentially equivalent to that measured by Komori et al., in which the VITA method is applied to concentration signals of dye tracer released from inside the turbulent boundary layer of the open channel. We also find that the constant for T_γ, $a = 0.20$, is very close to that reported by Kermani et al.,[16] $0.19 \lesssim a \lesssim 0.21$, at $Re_\tau \approx 300$ and $1 \leqq Sc \leqq 8$. In addition, it is observed that the ratio between T_S and T_γ appears to be approximately 2.6 at the Reynolds numbers that this study covered. The constant ratio T_S/T_γ suggests that the two characteristic time scales may have some possible physical relationship. Further scaling analysis for the two time scales is necessary to complete our goal of establishing a correlation between the turbulent scalar flux and the characteristic time scales at the free surface.

Future directions

Apart from future work on the scaling analysis of the two characteristic time scales, several topics remain to be comprehensively investigated. First, the effect of the Schmidt number on scalar flux at a free surface is not examined here. Instead of investigating the effect of the Schmidt number, we have focused our attention on the effect of the Reynolds number on scalar flux, and we have compared our results with those obtained from laboratory experiments. The effect of the Schmidt number is assumed to be $Sh \propto Sc^{1/2}$ based on several references.[12,13,16,17] Increasing the Schmidt number from the current value of 1 to, hopefully, $\mathcal{O}(10^2)$, is certainly called for in future work.

Second, this study parameterizes the hydrodynamic quantities using the wall-shear velocity, u_τ, water depth, δ, and fluid viscosity, ν. This paramerization is based on the fact that the flow field that we deal with here is a type of wall-bounded flow, so that these parameters are entirely appropriate. In several geophysical turbulent flows, nevertheless, a different parameterization may be required, as water depth in some cases is considered infinite. Perot and Moin[18] and Walker et al.[19] introduced different parameterizations of the hydrodynamics quantities under the assumption that turbulence is isotropic in a region away from a free surface.

Calmet and Magnaudet[12,13] used the velocity macro-scale and the integral length scale to normalize the hydrodynamic quantities. These parameterizations should be considered when trying to correlate the subsurface hydrodynamics and scalar transport at a free surface in turbulent environmental flows where the wall-shear velocity is difficult to define.

Finally, turbulent flows in this study deal with zero Froude and Weber numbers, hence deformation of the free surface by gravity and surface tension is not introduced. In some turbulent flows with a free surface, the Froude number is large as, for example, a liquid film flow along a wall or for a shallow geophysical flow. Also, for small-amplitude waves, the effect of the Weber number will play an important role. Many computational hurdles exist to deal with turbulent flows with the gas–liquid interface of nonzero Froude and Weber numbers. These problems include the descretization of the governing equations and their suitable boundary conditions. The availability of sufficient computational resources could also be an another hurdle. The inclusion of the effects of waves on turbulence and vise versa is clearly the most urgent problem requiring further research.

Acknowledgments

The authors express their appreciation to Professor Clive S. Langham of Graduate School of Dentistry, Nihon University, for his helpful comments throughout this manuscript.

Literature Cited

1. Komori S, Murakami Y, Ueda H. The relationship between surface-renewal and bursting motions in an open-channel flow. *J. Fluid Mech.* 1989;203:103–123.
2. Komori S, Nagaosa R, Murakami Y. Mass transfer into a turbulent liquid across the zero-shear gas-liquid interface. *AIChE J.* 1990;36:957–960.
3. Nagaosa R, Saito T. Turbulence structure and scalar transfer in stratified free-surface flows. *AIChE J.* 1997;43:2393–2404.
4. Nagaosa R. Direct numerical simulation of vortex structures and turbulent scalar transfer across a free surface in a fully developed turbulence. *Phys Fluids.* 1999;11:1581–1595.
5. Handler RA, Saylor JR, Leighton RI, Rovelstad AL. Transport of a passive scalar at a shear-free boundary in fully developed turbulent open channel flow. *Phys Fluids.* 1999;11:2607–2625.
6. Nagaosa R, Handler RA. Statistical analysis of coherent vortices near a free surface in a fully developed turbulence. *Phys Fluids.* 2003;15:375–394.
7. Dankwerts PV. Significance of liquid-film coefficient in gas absorption. *Ind Eng Chem.* 1951;43:1460–1467.
8. Rashidi M, Hetsuroni G, Banerjee S. Mechanisms of heat and mass transport at gas-liquid interfaces. *Int J Heat Mass Transfer.* 1991;34:1799–1810.
9. Rashidi M. Burst-interface interactions in free surface turbulent flows. *Phys Fluids.* 1997;9:3485–3501.
10. Kumar S, Gupta R, Banerjee S. An experimental investigation of the characteristics of free-surface turbulence in channel flow. *Phys Fluids.* 1998;10:437–456.
11. Pan Y, Banerjee S. A numerical study of free-surface turbulence in channel flow. *Phys Fluids.* 1995;7:1649–1664.
12. Calmet I, Magnaudet J. Statistical structure of high-reynolds-number turbulence close to the free surface of an open-channel flow. *J Fluid Mech.* 2003;474:355–378.
13. Magnaudet J, Calmet I. Turbulent mass transfer through a flat shear-free surface. *J Fluid Mech.* 2006;553:155–185.
14. Herlina, Jirka GH. Experiments on gas transfer at the air-water interface induced by oscillating grid turbulence. *J Fluid Mech.* 2008;594:183–208.
15. Janzen JG, Herlina H, Jirka GH, Schulz HE, Gulliver JS. Estimation of mass transfer velocity based on measured turbulence parameters. *AIChE J.* 2010;56:2005–2017.
16. Kermani A, Khakpour HR, Shen L, Igusa T. Statistics of surface renewal of passive scalars in free-surface turbulence. *J Fluid Mech.* 2011;678:379–416.
17. Wang L, Lu XY. Large eddy simulation of stably stratified turbulent open channel flows with low-to high-Prandtl number. *Int J Heat Mass Transfer.* 2005;48:1883–1897.
18. Perot B, Moin P. Shear-free boundary layers. Part 1. Physical insights into near-wall turbulence. *J Fluid Mech.* 1995;299:199–227.
19. Walker DT, Leighton RI, Garza-Rios LO. Shear-free turbulence near a flat free surface. *J Fluid Mech.* 1996;320:19–51.
20. Tamburrino A, Gulliver JS. Free-surface turbulence and mass transfer in a channel flow. *AIChE J.* 2002;48:2732–2743.
21. McKenna SP, McGillis WR. The role of free-surface turbulence and surfactants in air-water gas transfer. *Int J Heat Mass Transfer.* 2004;47:539–553.
22. Banerjee S, Lakehal D, Fulgosi M. Surface divergence models for scalar exchange between turbulent streams. *Int J Multiphase Flows.* 2004;30:963–977.
23. Hasegawa Y, Kasagi N. Hybrid DNS/LES of high Schmidt number mass transfer across turbulent air-water interface. *Int J Heat Mass Transfer.* 2009;52:1012–1022.
24. Smolentsev S, Miragharie R. Study of a free surface in open-channel water flows in the regime from "Weak" to "Strong" turbulence. *Int J Multiphase Flow.* 2005;31:921–939.
25. Shen L, Zhang X, Yue DKP, Triantafyllow G. The surface layer for free-surface turbulent flows. *J Fluid Mech.* 1999;386:167–212.
26. Enstad LI, Nagaosa R, Alendal G. Low shear turbulence structures beneath stress-driven interface with neutral and stable stratification. *Phys Fluids.* 2006;18:055106.
27. Choi H, Moin P. Effects of the computational time step on numerical solutions of turbulent flow. *J Comput Phys.* 1994;113:1–4.
28. Schumann U, Sweet RA. Fast Fourier transforms for direct solution of Poisson's equation with staggered boundary conditions. *J Comput Phys.* 1988;75:123–137.
29. Moser R, Kim J, Mansour NN. Direct numerical simulation of turbulent channel flow up to $Re_\tau = 590$. *Phys Fluids.* 1999;11:943–945.
30. McCready MJ, Vassiliadou E, Hanratty TJ. Computer simulation of turbulent mass transfer at a mobile interface. *AIChE J.* 1986;32:1108–1115.
31. Brumley BH, Jirka GH. Air–water transfer of slightly soluble gases: turbulence interfacial processes and conceptual models. *Physicochem Hydrodyn.* 1988;10:295–319.
32. Herlina, Jirka GH. Application of LIF to investigate gas transfer near the air–water interface in a grid-stirred tank. *Exp Fluids.* 2004;37:341–349.
33. Eckhardt B, Schumacher J. Turbulence and passive scalar transport in a free-slip surface. *Phys Rev E.* 2001;64:016314.
34. Bendat JS, Pearsol AG. *Random Data*, 2nd ed. New York, NY: Wiley, 2000.
35. Law CNS, Khoo BC. Transport across a turbulent air-water interface. *AIChE J.* 2002;48:1856–1868.

Manuscript received May 8, 2011, and revision received Jan. 31, 2012.